

# Linear Bayesian Filter based Low-cost UWB Systems for Indoor Mobile Robot Localization

Shuai Zhang, Ruihua Han, Wankuan Huang, Shuaijun Wang, Qi Hao\*

Department of Computer Science and Engineering

Southern University of Science and Technology

Shenzhen, Guangdong, 518055, China

Email: (zhangs6, hanrh, 11612501, wangsj)@mail.sustc.edu.cn, haoq@sustc.edu.cn, \*Corresponding author

**Abstract**—In this paper, we propose an improved UWB based indoor localization system using Bayesian filtering techniques. The system contains two key components: (1) miniaturized, high updating rate and highly reconfigurable UWB sensors with a linear regression model to calibrate range measurement errors; (2) a set of Bayesian filters which can improve the localization precision by utilizing the spatial correlation between the stationary UWB base stations and the mobile UWB station. Furthermore, a novel measurement transform is proposed to reduce the computational complexity. Experiments are performed in an indoor environment with the ground truth obtained by the motion capture system to validate and evaluate the proposed indoor localization system.

**Keywords**—Ultra-wideband (UWB); Bayesian Filter, Indoor localization.

## I. INTRODUCTION

In recent years, indoor localization becomes increasingly critical in many end-user applications such as indoor guidance, package tracking and surgery assistance [1] [2]. Various technologies have been developed for precise indoor localization, such as infrared, WIFI, Bluetooth, ZigBee, ultrasound, radio frequency identification (RFID), and ultra-wideband (UWB) [3]. The UWB technology is based on non-carrier communications and uses the narrow-pulse signal of nanosecond to transmit data, which provides the ultra-wideband signal with a high time resolution, yielding high positioning accuracy with low power consumption and low system complexity. As a result, the UWB technology is particularly suitable for reliable and accurate indoor real-time positioning [1].

Although the UWB technology has many strengths, its applications suffer from many technical challenges, including

- 1) possibility of interference with nearby RF systems [4],
- 2) time consuming processes for signal acquisition, synchronization and tracking with very high precision [5], and
- 3) technical difficulties from the design and implementation of the antennas for UWB systems [1].

Well-designed high-precision UWB systems can achieve superior localization performance at extra hardware costs [1] [3]. Besides, the UWB localization systems are based on

This work was supported by the Science and Technology Innovation Commission of Shenzhen Municipality (No. CKFW2016041415372174 and No. GJHZ20170314114424152), and the National Natural Science Foundation of China (No. 61773197).

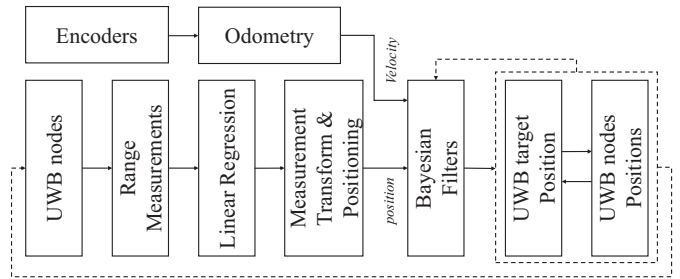


Fig. 1. Flowchart of low-cost localization system diagram.

range measurements and usually involve complicated filtering algorithms for target localization [2] [6] [7] [8].

In this paper, we develop a low-cost UWB system and utilize Bayesian filters to improve the accuracy of UWB localization, as shown in Fig. 1. To reduce the impact from measurement noise and system disturbances, the readings of both odometry and UWB modules are used to help localize mobile (target) and stationary (anchor) UWB module positions. The contributions of this work contain three folds:

- 1) developing low-cost UWB modules, which use a linear regression model to reduce the measurement errors;
- 2) developing a set of Bayesian filters, which localize the mobile and stationary UWB modules alternatively;
- 3) developing a nonlinear transform of measurements, which leads to linear filters with reduced computational complexity.

Besides, an experiment platform is developed with the motion capture system to provide the ground truth for system validation. The rest of the paper describes the self-developed UWB module, algorithm analysis and experimental evaluation.

## II. SYSTEM AND METHOD

### A. UWB Module Development and Calibration

Fig. 2 shows the snapshot of the developed UWB module.

This design can improve the performance of existing UWB modules and has a reduced size, multiple interfaces, high refresh rate, and high measurement precision. The UWB module mainly contains a control module (STM32F405RG), a power module (TPS73633\*2), a memory module (AT24C02), switches and a CAN bus interface (TJA1050). The advantages

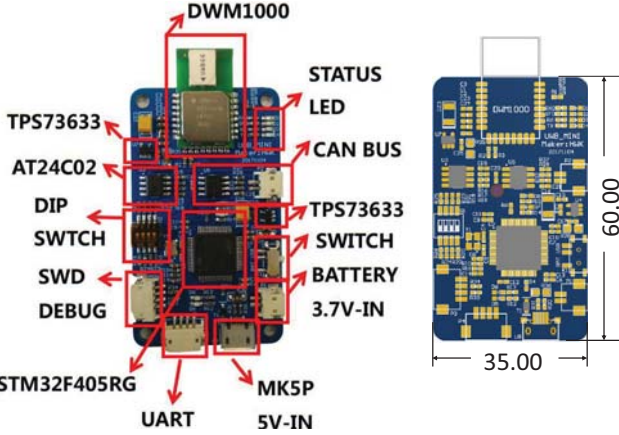


Fig. 2. Snapshot of the developed UWB module; Sensor Size: 35mm × 60mm.

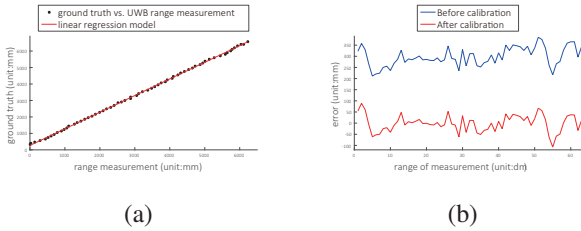


Fig. 3. (a) Linear regression model; (b) Error curves before and after calibration

of developed UWB module include: (1) a control module with a DSP unit and floating point parallel operations that can accelerate algorithms and improve the core working frequency; (2) UART serial and CAN controller LAN interfaces that enable fast configuration of the system parameters, and efficient transmission of data; and (3) a CAN bus architecture that enables communications between the UWB modules and high performance processors; and (4) digital switches that allow user to offline configure the IP address of the UWB module; and (5) flash memory units that can store UWB configuration data permanently, reducing the processing complexity.

As we can see from Fig. 3 (a), we create a linear curve fit to UWB range measurements and ground truth, the regression model is as the following:

$$f(x) = p_1x + p_2 \quad (1)$$

where  $p_1$  is linear factor and  $p_2$  is a constant. After calibration, as we can see from Fig. 3 (b), the max error and mean error of the UWB range measurement is reduced from 38.8cm to 10.7cm and 29.8cm to 3.0cm respectively, the corresponding RMSE after calibration is 3.8cm.

### B. Localization Problem Formulation

As we can see from Fig.4 (a), the UWB based indoor localization system consists of four anchor nodes and one target node whose position is to be determined,  $D_1$  to  $D_4$  are the range measurements that are conducted between anchor nodes and target node,  $h$  is the height from anchor node to the ground.

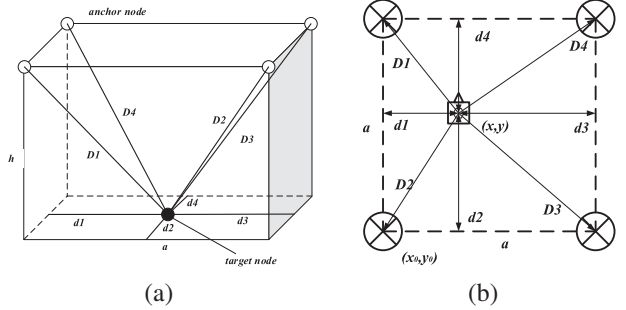


Fig. 4. (a) UWB based indoor localization 3D model; (b) UWB based indoor localization 2D model

Fig.4 (b) shows that  $d_1$  to  $d_4$  are the vertical distance from the node target to four boundaries of the bottom surface of space,  $a$  is the distance between two anchor nodes,  $x_0$  and  $y_0$  represent the left bottom vertex's coordinate. According to geometrical relationship,  $d_1$  to  $d_4$  can be calculated by measurement transform Eq.2 and they are linear dependent, which only have two independent elements and also represents a target's position,

$$\left\{ \begin{array}{l} d_1 = \frac{D_1^2 - D_2^2 + a^2}{2a} = x - x_0 \\ d_2 = \frac{D_2^2 - D_3^2 + a^2}{2a} = y - y_0 \\ d_3 = \frac{D_3^2 - D_4^2 + a^2}{2a} = -x + x_0 + a \\ d_4 = \frac{D_4^2 - D_1^2 + a^2}{2a} = -y + y_0 + a \end{array} \right. \quad (2)$$

As a result, the localization problem can be formulated in probabilistic terms:

$$p(u_{1:t}, m | z_{1:t}, \sigma_{1:t}) = p(m | z_{1:t}, u_{1:t}) p(u_{1:t} | z_{1:t}, m) p(u_t | u_{1:t-1}, m) \quad (3)$$

where  $u_{1:t} = [x_{1:t}, y_{1:t}]^T$  is the moving target's state vector from time 1 to  $t$  and  $x_t, y_t$  are the coordinates of moving target's position at time  $t$  in 2D model,  $m_t = [x_0 \ y_0 \ a]^T$  represents the 2D map,  $z_t = [d_{1t} \ d_{2t} \ d_{3t} \ d_{4t}]^T$  which represents the moving target's position that observed from the UWB modules at time  $t$ ,  $\sigma_{1:t}$  is the control vector from odometry reading.

### C. Bayesian Filtering for Localization

To improve positioning accuracy and reduce computation complexity, the moving target is assumed to be a constant velocity model and a set of bayesian filters is utilized to eliminate the common error by computing Eq.3.

Eq.4 illustrates the linear state transition function with added Gaussian noise,

$$u_t = Au_{t-1} + B\sigma_{t-1} + \varepsilon, \varepsilon \sim N(0, R) \quad (4)$$

where  $A$  is the state transition matrix which is a  $2 \times 2$  identity matrix,  $B$  is a  $2 \times 2$  identity matrix because of constant velocity input,  $\varepsilon_t$  is a  $2 \times 1$  process noise vector(zero mean multivariate normal distribution with covariance matrix  $R$  ).

As a result, priori estimate of the state  $\bar{u}_t$  and error covariance matrix  $\bar{\Sigma}_t$  calculated by the following Eq.5:

$$\left\{ \begin{array}{l} \bar{u}_t = Au_{t-1} + B\sigma_{t-1} \\ \bar{\Sigma}_t = A\Sigma_{t-1}A^T + R \end{array} \right. \quad (5)$$

Further more, observed value  $z$  at time  $t$  is as following:

$$z_t = Hu_t + Gm_t + v, v \sim N(0, Q) \quad (6)$$

Where  $z_t$  represents the moving target's position that observed from the UWB modules at time  $t$ .  $H$  and  $G$  are respectively the observation matrix and geometric transformation matrix, they represent the relationship between  $z$  and its current state  $u_t$ , surrounding environment map  $m_t$ ,  $v$  is a process noise vector(zero mean multivariate normal distribution with covariance matrix  $Q$ ). According to Eq.2,  $H$  and  $G$  are shown as following:

$$H = \begin{bmatrix} 1 & 0 \\ 0 & 1 \\ -1 & 0 \\ 0 & -1 \end{bmatrix}, G = \begin{bmatrix} -1 & 0 & 0 \\ 0 & -1 & 0 \\ 1 & 0 & 1 \\ 0 & 1 & 1 \end{bmatrix} \quad (7)$$

Based on Eq.6, the state vector and corresponding error covariance matrix  $\hat{u}_t \sim N(\hat{\mu}_t, \hat{\Sigma}_t)$  are estimated by Eq.8.

$$\begin{cases} \hat{\mu}_t = (H^T Q^{-1} H)^{-1} H^T Q^{-1} (z_t - Gm_t) \\ \hat{\Sigma}_t = (H^T Q^{-1} H)^{-1} \end{cases} \quad (8)$$

At the same time, more accurate map  $\hat{m}_t \sim N(\rho_t, M_t)$  is estimated by the following Eq.9:

$$\begin{cases} \rho_t = (G^T Q^{-1} G)^{-1} G^T Q^{-1} (z_t - Hu_t) \\ M_t = (G^T Q^{-1} G)^{-1} \end{cases} \quad (9)$$

Finally, estimation from Eq.5 and Eq.8 are combined by Eq.10 to further improve positional accuracy.

$$\begin{cases} \sum_t^{-1} = \hat{\sum}_t^{-1} + \bar{\sum}_t^{-1} \\ \sum_t^{-1} u_t = \hat{\sum}_t^{-1} \hat{u}_t + \bar{\sum}_t^{-1} \bar{u}_t \end{cases} \quad (10)$$

### III. EXPERIMENT RESULTS

Experiments are performed in an indoor environment with motion capture system as ground truth to validate the performance of localization system, see Fig. 5. The ground truth system consists of twelve *Prime17W* cameras and it can consistently produce positional error less than 0.3mm and rotational error less than 0.05. However, one of the limitations of ground truth is that the capture volume is  $11m \times 11m \times 3m$ . As a result, the experiments is limited to  $10m \times 10m$  and the ground truth system allows us to locate both the four UWB anchors and the mobile target with millimeter-level accuracy. The moving target with a UWB module is a ground mobile vehicle which contains an universal wheel chassis that can provide more precise odometer data.

Fig.6 shows the experiment results. The moving UWB target's trajectory comparison between ground truth and Bayesian based is shown in Fig.6 (a). The corresponding trajectory errors are shown in Fig.6 (b), it shows that the maximum localization error is 8.9cm and the mean error is 3.4cm, the RMSE is 0.1cm. Fig.6 (c) and (d) illustrate the dynamical update of map during the process of localization, the accuracy of  $x_0$ ,  $y_0$  and  $a$  are respectively kept within 2.6cm, 2.5cm

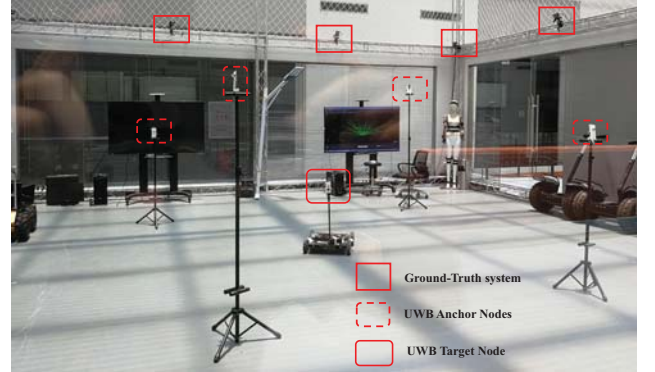


Fig. 5. UWB indoor localization experimental condition.

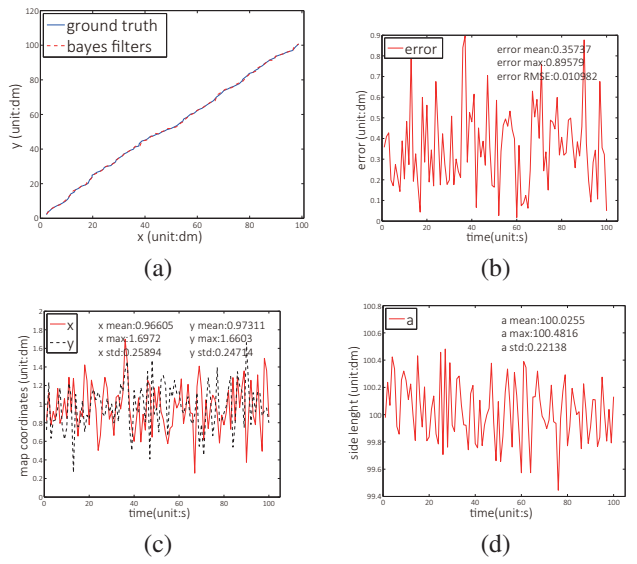


Fig. 6. Localization experiment results: (a) target's trajectory comparison between ground truth and bayesian filter based method; (b) localization error; (c)coordinates update for 2D map's left bottom vertex; (d) map update for 2D model's side length.

and 2.2cm, which indicates the high localization accuracy of proposed system.

### IV. CONCLUSION

This paper designs a low-cost UWB based localization system for mobile robot in indoor environment. The developed UWB module is upgraded in hardware, which can improve the performance of existing UWB modules in terms of size, configuration and working frequency. Meanwhile, a linear regression model is utilized to calibrate UWB range measurement errors and the UWB module can achieve a few centimeter of accuracy. To improve the developed system's localization precision, a measurement transformation algorithm is proposed to reduce the system's computation complexity and a set of linear Bayesian filters are utilized to optimize UWB target's positions and base nodes' precision. The integration of INS is under further development, and the performance of UWB based localization will be tested and be improved more in the future work.

## REFERENCES

- [1] A. Alarifi, A. Al-Salman, M. Alsaleh, A. Alnafessah, S. Al-Hadhrami, M. A. Al-Ammar, and H. S. Al-Khalifa, “Ultra wideband indoor positioning technologies: Analysis and recent advances,” *Sensors*, vol. 16, no. 5, p. 707, 2016.
- [2] J. Wang, Y. Tang, J.-M. Muñoz-Ferreras, R. Gómez-García, and C. Li, “An improved indoor localization solution using a hybrid uwb-doppler system with kalman filter,” in *Radio and Wireless Symposium (RWS), 2018 IEEE*. IEEE, 2018, pp. 181–183.
- [3] R. F. Brena, J. P. García-Vázquez, C. E. Galván-Tejada, D. Muñoz-Rodríguez, C. Vargas-Rosales, and J. Fangmeyer, “Evolution of indoor positioning technologies: A survey,” *Journal of Sensors*, vol. 2017, 2017.
- [4] R. Aiello and A. Batra, *Ultra wideband systems: technologies and applications*. Newnes, 2006.
- [5] D. Porcino and W. Hirt, “Ultra-wideband radio technology: potential and challenges ahead,” *IEEE communications magazine*, vol. 41, no. 7, pp. 66–74, 2003.
- [6] X. Cai, L. Ye, and Q. Zhang, “Ensemble learning particle swarm optimization for real-time uwb indoor localization,” *EURASIP Journal on Wireless Communications and Networking*, vol. 2018, no. 1, p. 125, 2018.
- [7] M. Ridolfi, S. Vandermeeren, J. Defraye, H. Steendam, J. Gerlo, D. De Clercq, J. Hoebeke, and E. De Poorter, “Experimental evaluation of uwb indoor positioning for sport postures,” *Sensors*, vol. 18, no. 1, p. 168, 2018.
- [8] Y. Wang and X. Li, “The imu/uwb fusion positioning algorithm based on a particle filter,” *ISPRS International Journal of Geo-Information*, vol. 6, no. 8, p. 235, 2017.